Predicting per capita expenditure using satellite imagery and transfer learning: A case study of east Java province, Indonesia

Heri Kuswanto[a*], Wahidatul Wardah Al Maulidiyah[a], Widhianingsih Tintrim Dwi Ary[a], Yudistira Ashadi[a]

[a]Department of Statistics, Institut Teknologi Sepuluh Nopember, Surabaya, Indonesia

CHRONICLE	ABSTRACT
	Collecting poverty data through the National Socio-Economic Survey (SUSENAS) demands significant time, costs, and human resources. To enable more efficient policy-making, predicting the poverty rate before the release of Statistics Indonesia (BPS) data is essential. This research compares day and night satellite images to predict per capita expenditure in East Java, Indonesia, which has the highest number of poor people. The satellite images are processed using a transfer learning approach that employs a pretrained Convolutional Neural Network (CNN) model with VGG-16 architecture as a feature extractor. These extracted features are then used as independent variables to predict East Java's per capita expenditure using Support Vector Regression (SVR) with RBF and polynomial kernels. The findings indicate that night images are more reliable than day images, with the best model being a combination of transfer learning and the SVR polynomial kernel using night images. The prediction mapping aligns well with the unmodeled night image, demonstrating the effectiveness of this approach in predicting per capita expenditure.

1. Introduction

Eradicating poverty is the first of the 17 Sustainable Development Goals (SDGs) to be achieved by 2030. As the primary goal, poverty eradication should be the central theme and sustainable agenda underpinning various development objectives, including infrastructure, tourism, food, energy, and more (Noor et al., 2008; Bappenas, 2022). According to BPS, poverty is defined using a basic needs approach, where individuals are considered poor if their average per capita expenditure falls below the poverty line. This data is derived from the National Socio-Economic Survey (SUSENAS). While survey-based data collection is accurate, it faces challenges such as high costs, the need for extensive human resources, and lengthy processing times, with estimates only available at the district/city level. To address these issues, BPS is integrating technology and utilizing big data sources, including day and night satellite imagery, to obtain faster and more accessible data. Predicting per capita expenditure using big data supports official statistics, allowing for estimations at smaller levels, which can facilitate quicker, data-driven government policies (Badan Pusat Statistik, 2022a).

Satellite imagery, including Nighttime Light (NTL) and daytime digital imagery, offers a novel data source for poverty mapping. Poverty identification can be enhanced through nighttime and daytime light analysis, which maps building characteristics, physical parameters such as road networks (access), and the shape and material of buildings. Daytime image analysis can also estimate slum levels (density and shape) and slum neighborhoods (location and environmental characteristics) (Badan Pusat Statistik, 2022b). Previous research using night imagery from the Defense Meteorological Satellite Program-Operational Linescan System (DMSP-OLS) sensor (Bhandari & Roychowdhury, 2011; Chen & Nordhaus, 2011) has shown a high correlation between night

imagery and population wealth, despite containing noise in low-economic areas. Research using daytime images has also been conducted with a transfer learning approach, producing high-dimensional features (Jean et al., 2016; Head, Manguin, Tran, & Blumenstock, 2017; Ngestrini, 2019; Rouhan, 2020). These features are then used as independent variables in regression modeling, including the Support Vector Regression (SVR) model. Night imagery is advancing with the Visible Infrared Imaging Radiometer Suite (VIIRS) sensor, which captures light more effectively. Previous studies (Aprianto, Wijayanto, & Pramana, 2022; Khairunnisah, Wijayanto, & Pramana, 2021) have utilized a combination of daytime and nighttime imagery from the VIIRS sensor, applying transfer learning and RBF kernel Support Vector Regression (SVR) in regression modeling. The type of kernel used in SVR significantly impacts model performance. Prior research (Moorthi et al., 2011; Ustuner, Sanli, & Dixon, 2017) indicates that polynomial kernels outperform RBF kernels for satellite image processing.

This study aims to predict per capita expenditure by comparing daytime and nighttime images (VIIRS NTL type) using the transfer learning approach with the VGG-16 architecture. Regression modeling is conducted with SVR, comparing the performance of RBF and polynomial kernels. The research focuses on East Java Province, which, as of March 2022, has the highest number of poor people in Indonesia. Accurate predictions in areas with high poverty can enhance government planning and efforts to reduce poverty.

2. Methods

2.1 Transfer Learning

Transfer learning involves using a pre-trained model by copying its parameters to solve similar tasks. These pre-trained models, such as ImageNet, VGGNet, and ResNet, are typically trained on large-scale datasets (Sewak, Karim, & Pujari, 2018). They serve as starting points in computer vision and programming to address computational challenges that require significant time and resources (Iriawan et al., 2020). In transfer learning, pre-trained models can be used as feature extractors or for fine-tuning existing models. As feature extractors, they provide row vector data. When fine-tuning, the pre-trained model is retrained with new data (Bunrit, Kerdprasop, & Kerdprasop, 2019; Smola & Scholkopf, 2004).
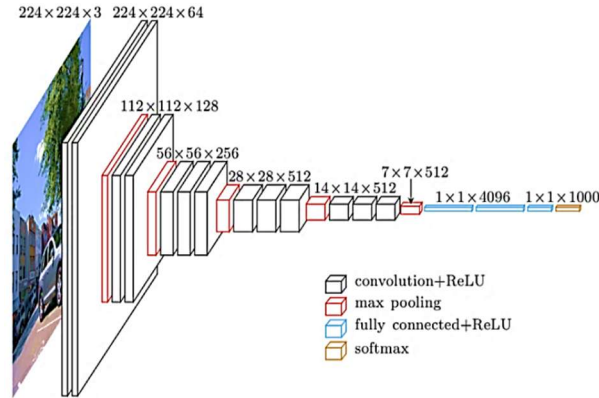

Fig. 1. Architecture of VGG-16 (Kamilaris & Prenafeta-Boldu', 2018)

VGG-16 is a CNN model architecture created by K. Simonyan and A. Zisserman from the University of Oxford in 2014 whose architectural arrangement is shown in Figure 1. This model was trained on 14 million images and 1000 classes. The VGG-16 architecture has 5 blocks consisting of 13 convolution layers and 3 fully connected layers. The input image in VGG-16 is 224×224×3 pixels for RGB images. The result obtained from the fully connected layer of this architecture is a 1×4096 vector which becomes the feature of the feature extraction process (Simonyan & Zisserman, 2015).

2.2 Support Vector Regression (SVR)

Support Vector Regression (SVR) is an application of Support Vector Machine (SVM) for regression cases. SVR aims to find *f(X)* as a hyperplane in the form of a regression function that fits the input data and produces the smallest possible error. SVR is good for high-dimensional datasets and non-linear cases using kernel functions. The regression function as the optimal hyperplane is written in Eq. (1) below,

$$f(X) = w^T \varphi(X) + b \tag{1}$$

where,

w: weighting parameter that has dimension

$\varphi(X)$: a function that maps to the feature space

b: bias

X: input vector

$f(X)$: regression function

coefficient w and b serve to minimize the risk function in Eq. (2) below.

$$R = min \left\{ \frac{1}{2} \|w\|^2 + C \frac{1}{l} \left(\sum_{i=1}^{l} L\varepsilon(Y_i f(X_i)) \right) \right\} \tag{2}$$

with the constraint function,

$$Y_i - w^T \varphi(X_i) - b \leq \varepsilon, \ \ w^T \varphi(X_i) - Y_i + b \leq \varepsilon, \ \ i = 1,2,\ldots,l \tag{3}$$

where,

$$L_{\varepsilon(Y_i, f(X_i))} = \begin{cases} 0, & untuk \ |Y - f(X)| < \varepsilon \\ |Y - f(X)| - \varepsilon, & untuk \ |Y - f(X)| \geq \varepsilon \end{cases} \tag{4}$$

L_ε : loss function with type

R : risk function

$\|w\|$: normalization

ε: deviation or degree of tolerance to error

C: penalty value if deviation exceeds

All points within the range $f(X) \pm \varepsilon$, are assumed to be feasible and vice versa. The optimization problem for feasible constraints is shown in Eq. (5)

$$F = min \frac{1}{2} \|w\|^2 \tag{5}$$

with the following constraint function,

$$Y_i - w^T \varphi(X_i) - b \leq \varepsilon, \ \ w^T \varphi(X_i) - Y_i + b \leq \varepsilon, \ \ i = 1,2,\ldots,l \tag{6}$$

Solving the infeasible condition problem is done by adding slack variables and the following Eq. (7).

$$IF = min \left\{ \frac{1}{2} \|w\|^2 + C \sum_{i=1}^{l} \left(\xi_i + \xi_i^* \right) \right\} \tag{7}$$

with restrictions,

$$Y_i - w^T \varphi(X_i) - b - \xi_i \leq \varepsilon,$$
$$w^T \varphi(X_i) - Y_i + b - \xi_i^* \leq \varepsilon, \tag{9}$$
$$\xi_i, \xi_i^* \geq 0; \ i = 1,2,\ldots,l.$$

So that the complete form of the dual SVR optimization problem in Eq. (9) is obtained as follows,

$$max \left\{ \frac{1}{2} \sum_{i,j=1}^{l} (\alpha_i - \alpha_i^*)(\alpha_j - \alpha_j^*)k(X_i, X_j) - \varepsilon \sum_{i,j=1}^{l} (\alpha_i - \alpha_i^*) + \sum_{i,j=1}^{l} Y_i(\alpha_i - \alpha_i^*) \right\} \tag{9}$$

with constraints (Hsu, Chang, & Lin, 2003),

$$\sum_{i,j=1}^{l}(\alpha_i - \alpha_i^*) = 0; \ 0 \le \alpha_i, \alpha_i^* \le C; \ i = 1,2,...,l \tag{10}$$

The application of kernel function in SVR is done to overcome the non-linear cases that often occur. The kernel function will transform the data in the non-linear input space into a high dimensional feature space. In this research, the kernel functions used are polynomial kernel and Radial Basis Function (RBF) kernel. The RBF Kernel formula can be written in Eq. (11),

$$k(X_i, X_j) = exp(-\gamma \|X_i - X_i\|^2) = exp\left(\frac{-\|X_i - X_j\|^2}{2\sigma^2} \right). \tag{11}$$

The polynomial kernel is a widely used kernel in image processing, especially image classification which can be shown in Eq. (12) below.

$$k(X_i, X_j) = \left(X_i^T X_j + c \right)^d, \tag{12}$$

where $i, j = 1, 2, ..., l$ with l is the number of support vectors (SV) and $d > 0$ is a constant (Karatzoglon, Smola, & Hornik, 2003).

2.3 Per Capita Expenditure

Per capita expenditure is the cost incurred for household consumption during the month divided by the number of household members and has been adjusted to purchasing power parity. The calculation of adjusted per capita expenditure is carried out using the formula in Eq. (13) which contains a constant price per capita expenditure component in Eq. (14).

$$Y_i = \frac{Y_i^*}{PPP_i} \tag{13}$$

$$Y_i^* = \frac{Y_i^{**}}{IHK} \times 100 \tag{14}$$

where

Y_i: i-th region adjusted per capita expenditure

Y_i^* : per capita expenditure at constant price of the i-th region

PPP_i : i-th district purchasing power parity

Y_i^{**}: annual per capita expenditure of the i-th region

IHK: consumer price index base year 2012.

2.4 Data and Data Sources

This research uses three types of data, namely adjusted per capita expenditure data for districts/cities in East Java in 2021 from BPS, daytime imagery from Google Maps, and nighttime imagery in the form of NTL VIIRS in 2021 from the Earth Observation Group (EOG) website.

Source: https://eogdata.mines.edu/
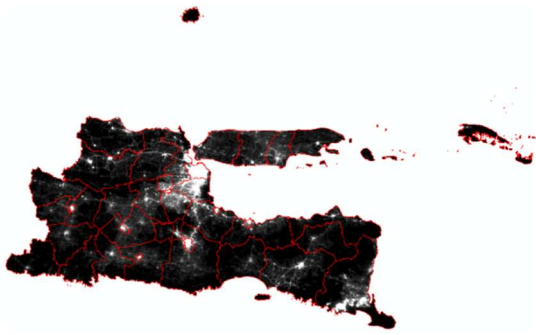
Fig. 2. Night Image of East Java 2021

Source: Google Maps

Fig. 3. Cropped Daylight Image of East Java 2022

The daytime imagery dataset comprises 94,539 image files captured at zoom level 16, each covering an area of approximately 1 km². Each image measures 400×400 pixels and was last taken on August 22, 2022. For this study, it is assumed that there are no significant changes in the imagery between 2021 and 2022. Retrieving the daytime imagery from Google Maps requires longitude and latitude data for each district/city and shapefiles (SHP) to delineate the boundaries of the 38 districts/cities in East Java.

Table 1
Research Data Structure

Regional	Y	X_1	X_2	X_3	$X_{...}$	X_{4096}
1	Y_1	$X_{1,1}$	$X_{2,1}$	$X_{3,1}$	…	$X_{4096,1}$
2	Y_2	$X_{1,2}$	$X_{2,2}$	$X_{3,2}$	…	$X_{4096,2}$
⋮	⋮	⋮	⋮	⋮	⋮	⋮
38	Y_{38}	$X_{1,38}$	$X_{2,38}$	$X_{3,38}$	…	$X_{4096,38}$

Per capita expenditure is the dependent variable, while the results of feature extraction serve as the independent variables. Feature extraction is conducted on each image within a folder designated for each district/city. Using the VGG-16 model, each image is processed to produce 4096 features. Since each region has multiple images, the average value of each feature is calculated, resulting in a 1×4096 dimensional data set for each district/city. East Java has 38 districts/cities, so the complete extraction results in a 38×4096 dimensional data set. Table 1 presents this data structure, which is used for SVR modeling

2.5   Analysis Step

The analysis involved comparing the use of nighttime and daytime images and evaluating the performance of RBF and polynomial kernels in SVR. Per capita expenditure data was explored statistically using boxplots and geographically using thematic maps, with the same methods applied to the prediction or estimation results. Night image cropping was conducted using a 1×1 km² grid. The best model was selected based on the highest R-value and the lowest MAPE value.

3. Result and Discussion

3.1 Characteristic of East Java Per Capita Expenditure

The average per capita expenditure in East Java is Rp 11,568,530 per year, which is higher than Indonesia's national average of Rp 11,013,000. Among East Java's 38 regions, 22 have below-average per capita expenditure. Bangkalan has the lowest per capita expenditure at Rp 8,673,000 per person per year, while Surabaya has the highest at Rp 17,862,000. Fig. 7 presents the geographical distribution of per capita expenditure across East Java's districts/municipalities. Different colors on the map represent quintiles, dividing the per capita expenditure into five categories. The darkest color represents the lowest quintile, comprising 8 regions. The second quintile includes 7 regions, the third quintile 8 regions, the fourth quintile 7 regions, and the brightest color indicates the highest quintile, consisting of 8 regions. Surabaya has the highest per capita expenditure due to its status as the provincial

capital and a hub for economy, education, government, and industry. Neighboring regions like Gresik and Sidoarjo also have high per capita expenditure, benefiting from their proximity to Surabaya and their roles in supporting its activities.

3.2 Estimation of Per Capita Expenditure using Daylight Satellite Imagery

Table 2
Parameters of SVR Model on Daylight Image

Parameters	RBF kernel		Polynomial kernel	
	Minimum	Maximum	Minimum	Maximum
Sigma	3.8×10^{-5}	6.7×10^{-4}	1.1×10^{-5}	1.95
C	0.032	1004.28	0.03	1021.06
R^2	38.78%	64.55%	35.75%	69.39%
Degree	-	-	1	3
MAPE	1.74%	13.59%	1.74%	13.97%

Feature extraction using VGG-16 yields a 38×4096-dimensional dataset, which serves as the independent variables, with per capita expenditure data as the dependent variable. Before modeling with SVR, it was observed that some of the 4096 extracted features were zero for all observations. Following the approach of prior research (Rouhan, 2020), these constant features were eliminated, as they are unsuitable predictors. In an equation $Y = f(X)$, X is constant or zero for all observations, Y would be the same for all observations. In the daytime image dataset, 26 variables were found to be constant or zero. Retaining these would negatively affect model performance. After eliminating these 26 features, SVR modeling was conducted with 4070 independent variables and one dependent variable. The dataset was divided into training and test sets using 10-fold cross-validation, and 400 hyperparameters were generated through random search for both the RBF and polynomial kernel SVR models, as shown in Table 2. The polynomial kernel outperformed the RBF kernel, achieving a maximum R^2 value of 69.39% with a MAPE of 1.91%. The smallest MAPE, 1.74%, corresponded to an R^2 value of 66.77%.

3.3 Estimating Per Capita Expenditure Using Nighttime Satellite Imagery

The estimation of per capita expenditure using night imagery follows similar steps to those used with daytime imagery but includes an additional step. This step involves cutting the night image according to a 1×1 km² SHP grid. To ensure that the grid edges align with the shape of each region's SHP, clipping is performed using ArcGIS software. The night imagery pieces are then created based on each region's SHP grid, resulting in TIF format images that match the grid cells for each region. To input these images into VGG-16, the TIF images are converted to JPG format and resized to 224×224 pixels. This process is repeated iteratively for each of the 38 district/city folders in East Java.

Table 3
Parameters of SVR Model on Night Image

Parameters	RBF kernel		Polynomial kernel	
	Minimum	Maximum	Minimum	Maximum
Sigma	5.3×10^{-6}	6.8×10^{-2}	1×10^{-5}	1.87
C	0.03	967.06	0.03	1016.61
Degree	-	-	1	3
R^2	53.25%	69.98%,	55.9%	87.05%
MAPE	1.67%	14%	1.85%	13.93%

3.4 Best Model Selection

A combination of modeling approaches was used, involving RBF kernel SVR and polynomial kernel SVR for both day and night images. All models utilized VGG-16 for feature extraction without altering its architecture or parameters. Parameter optimization was conducted by generating 400 hyperparameters through random search. The best parameters for each model are presented in Table 4.

Table 4
Parameters for Each Model

Model	*C*	*Sigma*	*Scale*	*Degree*
SVR RBF Daylight Image	9.1	8.9×10^{-5}		
Polynomial SVR Daylight Image	176.4		1×10^{-3}	2
SVR RBF Night Image	502.44	5.9×10^{-4}		
Night Image Polynomial SVR	**253.82**		8.3×10^{-1}	**2**

Fig. 4 shows that the overall MAPE for all models is less than 10%, indicating that all models exhibit high accuracy in predicting (Lewis, 1982). Among the models, the night image (in the figure denoted by Citra Malam) model with a polynomial kernel demonstrates the highest performance, while the RBF kernel model for the daytime image (in the figure denoted by Citra Siang) shows the lowest performance. This discrepancy is likely due to the greater color and object variations present in daytime images, making them more complex for the model to learn and recognize. In contrast, night images primarily consist of black, white, and gradients between these colors, offering fewer variations for the model to process, thus enhancing performance when applied to night images.
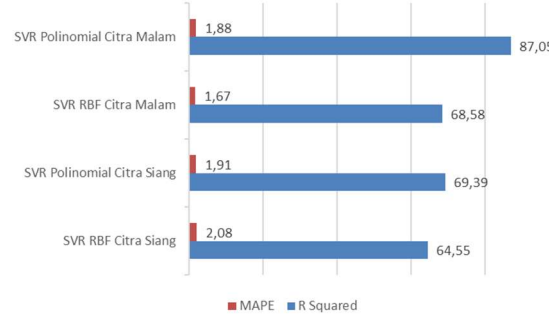

Fig. 4. Comparison of SVR Performance of All Models

The different kernels applied in SVR modeling significantly impact model performance. As shown in Fig. 4, the polynomial kernel outperforms the RBF kernel for both day and night images. This superiority is likely due to the polynomial kernel's more complex parameters, including the degree parameter, which optimizes values for each dataset, whether for day or night images. Table 4 reveals that for the polynomial kernel, the optimal degree for both day and night images is 2. Increasing the degree does not necessarily enhance model performance and requires longer running times (Diani, Wisesty, & Aditsania, 2017). VGG-16, originally trained using ImageNet data, has been applied to health data from X-ray or MRI and to road sign recognition for moving vehicles (Simonyan & Zisserman, 2015). These data characteristics are similar to the pattern of remote sensing data, such as satellite imagery that captures small objects. The feature extraction results from satellite images using VGG-16, which produce 38×4096 dimensional data, fall into the category of microarray data. For this type of data, SVR modeling with a polynomial kernel is more effective than with an RBF kernel. These findings are consistent with previous research (Diani, Wisesty, & Aditsania, 2017; Moorthi, Misra, Kaur, Darji, & Ramakrishnan, 2011; Ustuner, Sanli, & Dixon, 2017). The best performance among the four models is achieved by the SVR model with a polynomial kernel applied to night images. Although this model produces a larger MAPE compared to the RBF kernel SVR model on night images, it yields the highest R value, which is significantly higher than those of the other three models. The optimal polynomial kernel SVR model has an ϵ value of 0.1 and uses 32 support vectors (SVs). The relevant hyperparameters are detailed in Table 4, and the optimization problem for the best dual SVR model is expressed in Eq. (15).

$$max\left\{\frac{1}{2}\sum_{i,j=1}^{32}(\alpha_i-\alpha_i^*)(\alpha_j-\alpha_j^*)\text{k}(X_i,X_j)-0.1\sum_{i,j=1}^{32}(\alpha_i-\alpha_i^*)+\sum_{i,j=1}^{32}Y_i(\alpha_i-\alpha_i^*)\right\} \tag{15}$$

with restrictions,

$$\sum_{i,j=1}^{32}(\alpha_i-\alpha_i^*)=0;\ 0\le\alpha_i,\alpha_i^*\le253.82;\ i=1,2,...,32 \tag{16}$$

The optimal regression function from Eq. (15) is shown in Eq. (17).

$$f(x)=\sum_{i,j=1}^{32}(\alpha-\alpha^*)\text{k}(X_i,X_j) \tag{17}$$

$$\text{k}(X_i,X_j)=\left(X_i^TX_j+0.83\right)^2 \tag{18}$$

where *i, j* = 1,2,...,32 which is the number of SVs.

Based on the model performance for both day and night imagery, night imagery is more reliable than daytime imagery. Additionally, night imagery offers the advantage of easier data acquisition. Night imagery captured by the VIIRS sensor is freely available

on the EOG website, with a single file covering all regions of the earth in TIF format, available as annual or monthly data. In contrast, obtaining daytime imagery requires the use of the Google Map Application Programming Interface (API). Free usage of this API is limited by the number of images that can be downloaded. However, a significant advantage of daytime imagery is that it can be retrieved in real-time via Google Maps, allowing for more frequent updates and alignment with the latest conditions.

3.5 Mapping of Per Capita Expenditure Estimation Results

The mapping of per capita expenditure using the best model achieves an R^2 of 87.05% and a MAPE of 1.88%. According to research by Badan Pusat Statistik (2022a), prediction accuracy can also be indicated by the correlation value between actual data and prediction results; a higher correlation value signifies greater accuracy (Mukaka, 2012). The correlation between the prediction results and the actual data is 99.63%, as illustrated in Fig. 5. The percentage error, calculated as the difference between the actual and predicted values divided by the actual value, ranges from 0.52% to 2.56% for each region.
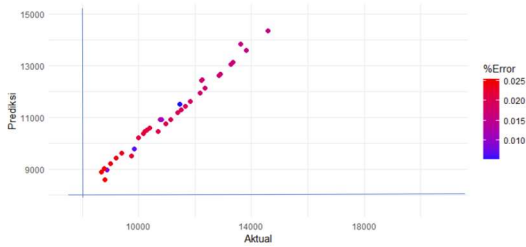

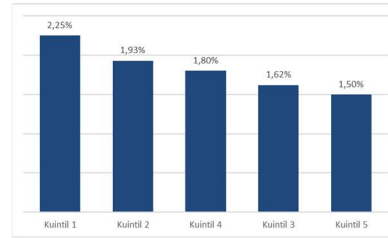**Fig. 5.** Correlation between Actual Data and Predicted Results

Fig. 6. Percentage of Prediction Error in Each District/City

The percentage error in terms of quintiles for each region reveals that quintile one has a larger percentage error compared to the other quintiles. Fig. 6 illustrates the average percentage error for each quintile, showing that quintiles one and two have the highest average percentage errors. In contrast, quintile five, representing the most prosperous regions, has the lowest average percentage error at 1.5%.
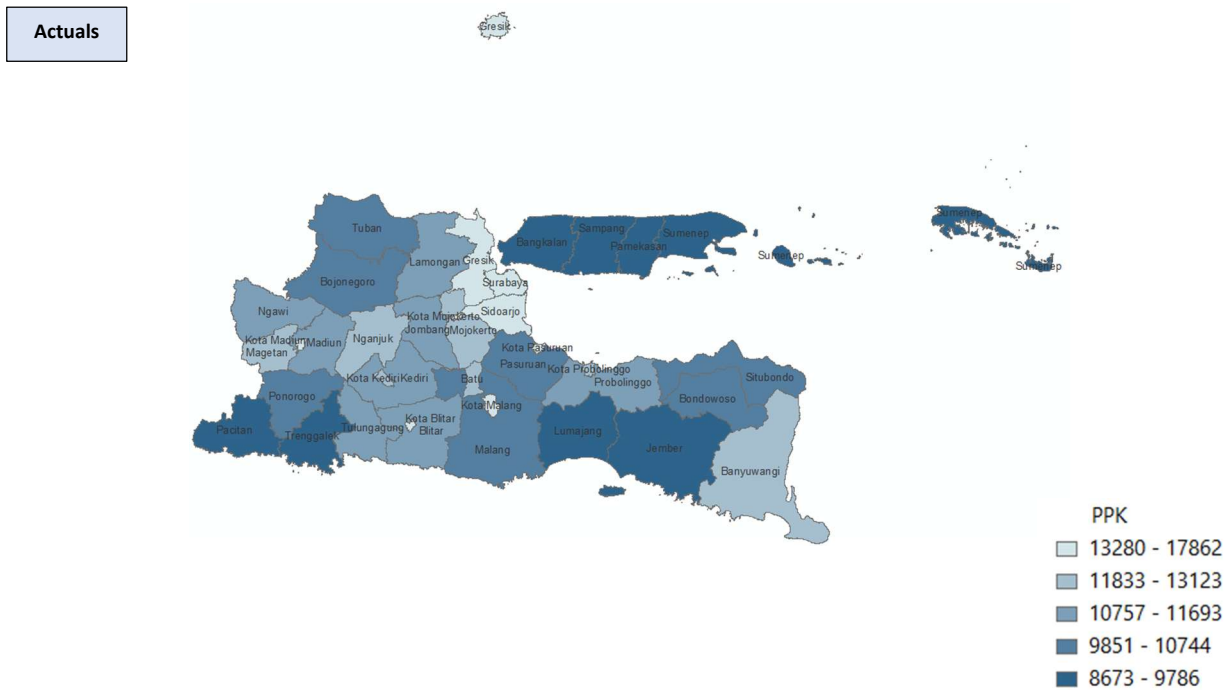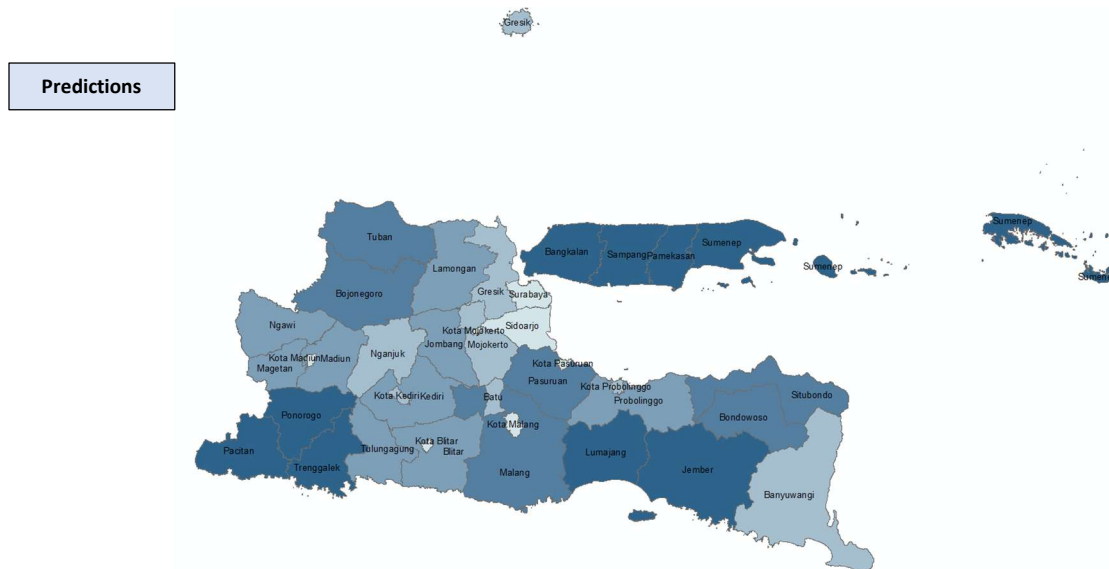
Fig. 7. Geographical Comparison of Predictions and Actuals

Per capita expenditure is less accurately predicted in areas with low light and economic intensity, particularly in quintile one. This aligns with findings from Badan Pusat Statistik (2022a) and Chen & Nordhaus (2011), which indicate that night imagery contains noise in low-economic areas. For example, the provinces of Papua and West Papua have the lowest poverty prediction performance due to their comparatively lower economic status. Geographically, the comparison of prediction results with actual data for East Java in 2021 is presented in Figure 7 according to the quintiles of per capita expenditure. The predictions achieve an accuracy rate of 92.11%, with the estimated per capita expenditure of 35 out of 38 districts/cities falling into the same quintile as the actual data. However, three districts show less precise estimates: Gresik, which is actually in quintile 5, is predicted to be in quintile 4; Magetan, which is actually in quintile 4, is predicted to be in quintile 3; and Ponorogo, which should be in quintile 2, is predicted to be in quintile 1. These areas are underestimated, although they still have a percentage error of less than 2%. The predicted per capita expenditure for each district/city correlates well with the unmodeled night imagery. The night image slice for East Java in Fig. 2, which includes red borders to show district/city boundaries, indicates that brighter areas correspond to higher light intensity and, thus, higher economic activity. Surabaya and its surrounding areas, predicted to have a high average per capita expenditure, exhibit high night light intensity, appearing bright white in Figure 2. This pattern holds true for other urban areas, such as Malang city and Batu city, which are also indicated by bright white circles within their respective smaller SHP boundaries. Extraction of night light intensity values from Fig. 2 can also be performed using ArcGIS software. The extracted value represents the average light intensity per region from a 1×1 km² grid, clipped to the shape of the East Java SHP. Surabaya city, Mojokerto city, and Malang city exhibit higher average night light intensities compared to other areas, significantly exceeding the average night light intensity of East Java, which is 3.85 radiance. This high intensity leads the model to predict these three regions to be in the highest per capita expenditure quintile, quintile 5. Conversely, Pacitan has the lowest night light intensity, with an average value of 0.35 radiance, which is below the East Java average. This condition results in both the actual and predicted classification of Pacitan falling into quintile 1 for per capita expenditure.

4. Conclusions

Based on the discussion, it is concluded that East Java has a higher average per capita expenditure than Indonesia, with a value of Rp 11,568,530 per person per year. Surabaya boasts the highest per capita expenditure in East Java at Rp 17,862,000, while Bangkalan Regency has the lowest at Rp 8,673,000. Predictions of per capita expenditure using night imagery are more reliable than those using daytime imagery. Additionally, the polynomial kernel in SVR proves to be more effective for satellite image processing than the RBF kernel. The best model, which combines a transfer learning model with polynomial kernel SVR using night imagery, achieves an R^2 of 87.05% and a MAPE of 1.88%. This model's predictions align well with actual quintile data, reaching an estimation accuracy of 92.11%. Furthermore, the prediction mapping is consistent with the unmodeled night image, where areas with higher brightness levels correspond to higher per capita expenditure prediction.

Acknowledgements

References

Aprianto, K., Wijayanto, A., & Pramana, S. (2022). Deep Learning Approach using Satellite Imagery Data for Poverty Analysis in Banten, Indonesia. *IEEE International Conference on Cybernetics and Computational Intelligence,* doi: 10.1109/cyberneticscom55287.2022.9865480.

Badan Pusat Statistik. (2022a). *Teknik Pengumpulan Data dan Preprocessing Citra Satelit.* Jakarta: Badan Pusat Statistik.

Badan Pusat Statistik. (2022b). *Pemodelan Citra Malam untuk Estimasi Kemiskinan Desa*. Jakarta: Badan Pusat Statistik.

Bappenas. (2022). *Tujuan Pembangunan Berkelanjutan.* Diambil 21 Juni 2022, dari https-://sdgs.bappenas.go.id/tujuan-1/

Bhandari, L., & Roychowdhury, K. (2011). Night lights and economic activity in India: A study using DMSP-OLS night time images. *Proceedings of the Asia Pacific Advanced Network* (pp. 218-236). doi: 10.7125/apan.32.24.

Bunrit, S., Kerdprasop, N., & Kerdprasop, K. (2019). Evaluating on the Transfer Learning of CNN Architectures to a Construction Material Image Classification Task. *International Journal of Machine Learning and Computing*, 9(2), doi: 10.18178/-ijmlc.2019.9.2.787.

Chen, X., & Nordhaus, W. (2011). Using luminosity data as a proxy for economic statistics. PNAS (*Proceedings of the National Academy of Sciences*), 8589-8594. https://doi.org/-10.1073/pnas.1017031108

Diani, R., Wisesty, U. N., Aditsina, A. (2017) Analisis Pengaruh Kernel Support Vector Machine (SVM) pada Klasifikasi Data Microarray untuk Deteksi Kanker. *IndoJC (Indonesian Journal of Computing)*, 2(1), 109-118

Head, A., Manguin, M., Tran, N., & Blumenstock, J. (2017). Can Human Development be Measyred with Satellite Imagery ? ICTD, https://doi.org/10.1145/3136560.3136576.

Hsu, C.-W., Chang, C.-C., & Lin, C.-J. (2003). A Practical Guide to Support Vector Classification. *Department of Computer Science, National Taiwan University*, http://-www.csie.ntu.edu.tw/~cjlin.

Iriawan, N., Pravitasari, A., Almuhayar, M., Azmi, T., Irhamah, Fithriasari, K., . . . Ferriastuti, W. (2020). UNet-VGG16 with transfer learning for MRI-based brain tumor segmentation. TELKOMNIKA *Telecommunication, Computing, Electronics and Control*, 1310-1318.

Jean, N., Burke, M., Xie, M., Davis, M., Lobell, D., & Ermon, S. (2016). Combining satellite imagery and machine learning to predict poverty. *Science 353*, DOI: 10.1126/-science.aaf7894.

Karatzoglon, A., Smola, A., & Hornik, K. (2003). *kernlab – An S4 Package for Kernel Methods in R*. Diambil dari kernlab–A Kernel Methods Package: https://www.-semanticscholar.org/paper/kernlab

Khairunnisah, Wijayanto, A., & Pramana, S. (2021). *Poverty Prediction and Mapping on Urban Areas using VIIRS Night-time Light Satellite Imagery Data (Case Study: Yogyakarta, Indonesia).* Jakarta: Politeknik Statistika STIS.

Lewis, C. (1982). *International and Business Forecasting Methods*. London: Butterworths.

Moorthi, M., Misra, I., Kaur, R., Darji, N., & Ramakrishnan, R. (2011). Kernel based learning approach for satellite image classification using support vector machine. *IEEE*, 107-110.

Mukaka, M. M. (2012). Statistics corner: A Guide to Appropriate Use of Correlation Coefficient in Medical Research. *Malawi Med* J. 69-71.

Ngestrini, R. (2019). Predicting Poverty of a Region from Satellite Imagery using CNNs. *Utrecht University*.

Noor, A. M., Alegana, V. A., Gething, P. W., Tatem, A. J., & Snow, R. W. (2008). Using Remotely Sensed Night-time Light as a Proxy for Poverty in Africa. *Population Health Metrics*, 6, https://doi.org/10.1186/1478-7954-6-5

Rouhan, A. (2020). *Prediksi Pengeluaran Perkapita yang Disesuaikan Berdasarkan Citra Digital Google Earth Menggunakan Kombinasi Convolutional Network (CNN) dan Support Vector Regression (SVR).* Surabaya: Institut Teknologi Sepuluh Nopember.

Sewak, M., Karim, M., & Pujari, P. (2018). *Practical Convolutional Neural Network* (I ed.). Birmingham: Packt Publishing Ltd.

Simonyan, K., & Zisserman, A. (2015). Very Deep Convolutional Networks for Large-Scale Image Recognition. *ICLR*(https://www.robots.ox.ac.uk/~vgg/research/very_deep/).

Smola, A., & Scholkopf, B. (2004). A tutorial on support vector regression. *Statistics and Computing*, 199-222.

Ustuner, M., Sanli, F., & Dixon, B. (2017). Application of Support Vector Machines for Landuse Classification Using High-Resolution RapidEye Images: A Sensitivity Analysis. *European Journal of Remote Sensing*, https://doi.org/10.5721/EuJRS20154823.